Theor Appl Climatol (2012) 108:135–145
DOI 10.1007/s00704-011-0520-y

ORIGINAL PAPER

On the relationship between the Bowen ratio and the near-surface air temperature

Jaeil Cho · Taikan Oki · Pat J.-F. Yeh · Wonsik Kim · Shinjiro Kanae · Kyoichi Otsuki

Received: 21 November 2010 / Accepted: 30 August 2011 / Published online: 10 September 2011

Abstract The sensitivity of land surface energy partitioning to near-surface air temperature (T_a) is a critical issue to understand the interaction between land surface and climatic system. Thus, studies with in situ observed data compiled from various climates and ecosystems are required. The relations derived from such empirical analyses are useful for developing accurate estimation methods of energy partitioning. In this study, the effect of T_a on land surface energy partitioning is evaluated by using flux measurement data compiled from a global network of eddy covariance tower sites (FLUXNET). According to the analysis of 25 FLUXNET sites (60 site-years) data, the Bowen ratio is found to have a linear relation with the bulk surface resistance normalized by aerodynamic and climatological resistance parameters in general, of which the slope and intercept are dependent on T_a. Energy partitioning in warmer atmosphere is less sensitive to changes in land surface conditions. In addition, a negative relation is found between Bowen ratio and T_a, and this relation is stronger above less vegetated surface and under low vapor pressure deficit and low received radiative energy condition. The empirical results obtained in this study are expected to be useful in gaining better understanding of alternating surface energy partitioning under increasing T_a.

J. Cho (✉) · K. Otsuki
Kasuya Research Forest, Kyushu University,
Sasaguri,
Fukuoka 811-2415, Japan
e-mail: chojaeil@gmail.com

T. Oki · P. J.-F. Yeh
Institute of Industrial Science, The University of Tokyo,
4-6-1 Komaba, Meguro-ku,
Tokyo 153-8505, Japan

W. Kim
National Institute for Agro-Environmental Sciences,
3-1-3 Kannondai,
Tsukuba 305-8604, Japan

S. Kanae
Department of Mechanical and Environmental Informatics,
Tokyo Institute of Technology,
2-12-1 O-okayama, Meguro-ku,
Tokyo 152-8552, Japan

1 Introduction

A biosphere–atmosphere coupling, which determines the steady state of the atmosphere to a large extent (Beljaars and Holtslag 1991), is closely related to the energy partitioning between latent heat flux (LE) and sensible heat flux (H) on the land surface (Henderson-Sellers et al. 1993; Wilson et al. 2002). Energy partitioning at the land surface is a complex function across different climate zones and ecosystems. Variations in the biological, land surface, and meteorological factors considerably influence surface partitioning of available energy. Monteith (1965) proposed that the leaf stomatal response and total green leaf area can be used to determine flux partitioning of incoming radiative energy. A numerical experiment conducted by Kondo et al. (1990) showed that the ground soil is apparently linked to the atmosphere by water vapor diffusion and heat conduction, and the behavior is highly dependent on soil properties (Mölders 2005). However, Jarvis et al. (1976) suggested that the difference in observed Bowen ratio (β, the ratio of H to LE) among crop fields is largely due to concomitant differences in the climatological factors such as temperature and water vapor.

Temperature is one of the most important climatological factors in the system of biosphere–atmosphere interaction. Near-surface air temperature (T_a) has an influence on the fluxes of radiant energy transfer, H between the surface and surrounding atmosphere, LE from or to the surface, and surface/subsurface heat storage (Jarvis et al. 1976; Wilson et al. 2002). These influences of T_a are significant on the atmospheric circulation. Both observations and climate modeling results indicate that global T_a has increased with time (Trenberth et al. 2007), and this trend will continue in the future (Randall et al. 2007). Additionally, T_a is most important variable in the terrestrial water cycle. For example, Komatsu et al. (2008) reported that evapotranspiration (ET) data observed in Japan show less clear correlation with precipitation than with temperature.

Thus, the sensitivity of energy partitioning to T_a is a critical issue to understand the interaction between the land surface and climatic system. Some previous studies based on direct measurements (e.g., Chang and Root 1975; Brutsaert 1982; Wilson et al. 2002) have related the characteristics of surface energy partitioning with T_a. However, in situ observed data compiled from diverse climates and ecosystems are still rare though they are most helpful to gain general understanding (Baldocchi and Meyers 1998; Beringer et al. 2005; Komatsu et al. 2008). Empirical relationships derived from such data analyses are important in the development of accurate estimation methods of land surface energy partitioning.

Wilson et al. (2002) presented flux measurement data collected from a global network of eddy covariance tower sites (FLUXNET: Baldocchi et al. 2001). In this study, we evaluate the effects of T_a on surface energy partitioning using the compiled data by Wilson et al. (2002). The result achieved through this kind of analysis would be useful in gaining general understanding of alternating surface energy partitioning under increasing T_a. This paper is organized into five sections. Section 2 describes the observed FLUXNET data of Wilson et al. (2002). Section 3 provides theoretical background and literature review related to land surface energy partitioning. The analysis results obtained by using the FLUXNET data in comparison with previously derived theoretical or empirical equations in literature are presented in Section 4, and it will be followed by the conclusions in Section 5.

2 Theoretical background

2.1 Resistance parameters

The influence of surface and atmospheric variables on the partitioning of available energy can be analyzed by evaluating the following three components of resistance: the aerodynamic, bulk surface and climatological resistance, denoted by R_a, R_s, and R_i, respectively (Jarvis et al. 1976; Brutsaert 1982). R_s, R_a, and R_i are generally used individually as separate parameters in the model of evapotranspiration from land surface to the atmosphere (see the discussion in Section 2.3). However, these three resistance parameters affect each other by the indirect or feedback responses as indicated by the (long dotted-dashed) arrows in Fig. 1.

The aerodynamic resistance (R_a) is a function of the water vapor, heat, and momentum transport in the near-surface boundary layer affected by near-surface aerodynamic and thermal properties. Thus, it is related to wind speed, the aerodynamic roughness of the vegetation, and the stability of the atmosphere. The bulk surface resistance (R_s) is a function of water vapor transport from the land surface to atmosphere. This transport mechanism is, in turn, controlled by the leaf stomata (responsible for plant transpiration) and soil water source (responsible for soil surface evaporation) because it conceptually implies bulk stomatal resistance of the canopy, bulk boundary layer resistance of the vegetation, bulk ground resistance, and bulk boundary layer resistance of the ground. The climatological resistance (R_i)

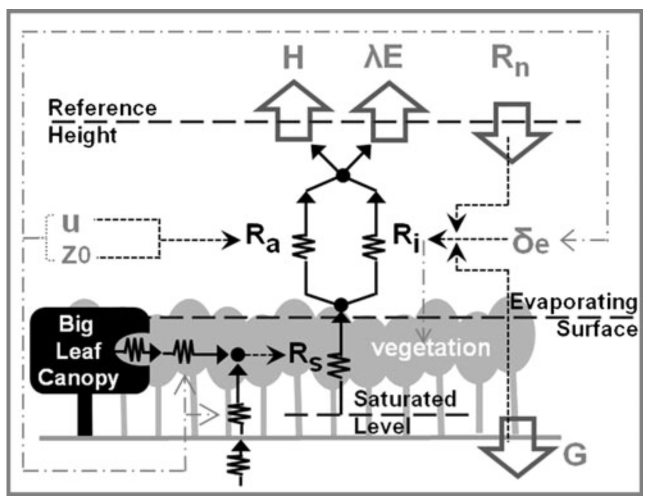

Fig. 1 A diagram showing the influence of three resistance parameters in the Penman–Monteith big-leaf method (Eq. 3) to surface energy partitioning: bulk surface resistance (R_s), climatological resistance (R_i), and aerodynamic resistance above the canopy (R_a). R_s is function of water vapor transport from the surface to the atmosphere. R_i is changed by available energy (R_n–S–G) and atmospheric vapor pressure deficit (δ_e). R_a is mainly determined by wind speed (u) and surface aerodynamic roughness (z_0). *Solid arrow lines* are the vapor transfer flow. *Dashed arrow lines* are direct environmental control. *Long dashed-dotted arrow lines* are indirect environmental control. See Brutsaert (1982) and Bonan (2002) for detailed understanding of this diagram

cannot be identified at a specific point in the soil–plant–atmosphere continuum. Instead, it is the ratio of atmospheric vapor pressure deficit (δ_e) to surface available energy with the same unit (s m^{-1}) as other resistance parameters.

$$R_i = \frac{\rho C_p \delta_e}{\gamma (R_n - S - G)} \tag{1}$$

where ρ is the density of air (kg m^{-3}), C_p is the specific heat capacity of moist air at constant pressure (J kg^{-1}°C^{-1}), γ is the psychrometer constant (Pa°C^{-1}), R_n is net radiation, and S and G are the change in the heat storage capacity within the soil and canopy, respectively. Evaporation moistens the atmosphere and its intensity depends on the atmospheric demand for water. However, atmospheric drying can occur due to mixing of dry air, despite the ample supply of moisture from the surface. R_i has been historically discussed to describe the feedback on evaporation (Thom 1975). Generally, R_i is high if δ_e is large (as an indicative of a dry atmosphere) or if available energy (A=R_n–S–G) is small (DeHeer-Amissah et al. 1981). Thus, R_i is a suitable parameter to be used to examine climatic control on energy partitioning (Wilson et al. 2002).

2.2 Previous flux measurement studies

Previous flux measurement studies have reported that the relative partitioning of A into LE and H is generally governed by climatic and surface conditions (Brutsaert 1982; Bonan 2002). Chambers et al. (2005) showed that the relative partitioning of R_n is influenced by surface characteristics such as albedo, surface roughness length, and surface temperature. Hammerle et al. (2008) reported that albedo, which is reduced by surface greenness, affects the amount of partitioned energy available to the ecosystem, and that surface energy partitioning is predominantly a function of LE. Admiral et al. (2006) reported that the increased A and δ_e causes an increase in LE, especially when R_n is within the range of 400–550 Wm^{-2}, and the soil moisture is physiologically sufficient. Therefore, the sensitivity of surface energy partitioning to temperature under warming condition may change with respect to different climates and vegetated surfaces.

The variability in the energy partitioning in various terrestrial ecosystems has also been investigated by using the estimated β and resistance parameters R_a, R_s, and R_i in previous various flux measurement studies (e.g., Wilson et al. 2002; Beringer et al. 2005; Chambers et al. 2005). Beringer et al. (2005) noted the changes in R_s and R_a when altering vegetation structure through dynamic transition from tundra to forest, and these characteristics control the land surface energy balance. Wilson et al. (2002) quantified LE by using three resistance parameters (R_a, R_s, and R_i) and found the differences in energy partitioning are mainly due to the differences in R_s and R_i among various vegetation types. These results signify that it is necessary to analyze the influence of three resistance parameters on the surface energy partitioning.

2.3 Evapotranspiration models

As a linkage between the atmosphere and land surface, evapotranspiration ET (as a representative of LE), serves as a key regulator of surface energy partitioning processes. Equilibrium evapotranspiration (ET_{equ}) indicates the lower limit of evaporation from a wet surface under the condition of minimal advection (Raupach 2000; Monteith and Unsworth 2008), and it is a function of A and T_a (Baldocchi 1994):

$$\lambda ET_{equ} = \frac{\Delta}{\Delta + \gamma}(R_n - S - G) \tag{2}$$

where λ is the latent heat of water vaporization (J kg^{-1}), and Δ is the slope of the saturation vapor pressure curve with respect to temperature at a specified temperature (Pa°C^{-1}). Under the ET_{equ} condition, the fraction of available energy used for latent heat evaporation is determined by the value of $\Delta/(\Delta+\gamma)$, approximately equal to 40% at 0°C, 56% at 10°C, 69% at 20°C, 79% at 30°C, and 86% at 40°C (Chang and Root 1975).

Since ET_{equ} is commonly higher than the actual ET due to the resistances between the land surface and atmosphere, R_s and R_a have been introduced to relate ET_{equ} to the actual ET. One well-known formula is the following Penman–Monteith equation based on the big-leaf concept (Monteith 1995; also see Fig. 1) derived from both energy conservation principle (energy balance) and aerodynamic method (mass transfer):

$$\lambda ET = \frac{\Delta(R_n - S - G) + \rho C_p \delta_e / R_a}{\Delta + \gamma(1 + R_s/R_a)} \tag{3}$$

The Penman–Monteith equation embodies the physical (non-physiological) and the biological (physiological) factors to estimate actual ET (the sum of soil evaporation, interception evaporation, and canopy transpiration). The variable of R_s depends mainly on the vegetation surface condition (e.g., soil moisture and surface temperature) and plant physiology (e.g., stomatal behavior), and R_a is strongly controlled by wind speed and plant architecture.

2.4 Indicators for surface energy partitioning

The Priestley–Taylor equation (Priestley and Taylor 1972) relates the ratio of ET to ET_{equ} to the Priestley–Taylor coefficient (α):

$$\lambda ET = \alpha \lambda ET_{equ} \tag{4}$$

α is widely used to evaluate the evapotranspiration rate because it permits a comparison of the evapotranspiration data obtained under different meteorological conditions (Baldocchi et al. 2000; Komatsu 2005).

The Penman–Monteith equation (Eq. 3) has been algebraically inverted by Jarvis et al. (1976) to examine the relative control of available energy, atmospheric water vapor, and physiological resistance on evapotranspiration. Jarvis et al. (1976) expressed the Bowen ratio β as follows:

$$\beta = \frac{1 + (R_s/R_a) - (R_i/R_a)}{\varepsilon + (R_i/R_a)} \tag{5}$$

where ε (=Δ/γ) is a functional parameter depending on atmospheric temperature and water vapor. Further, α can be related to β by the following equation (Brutsaert 1982; Holtslag and Van Ulden 1983):

$$\alpha = \frac{1 + (1/\varepsilon)}{1 + \beta}, \ \beta = 1/\alpha\varepsilon + 1/\alpha - 1 \tag{6}$$

By following the big-leaf concept of the Penman–Monteith equation, α (or β) can be described by the meteorological factors and resistance parameters and can be used as an energy partitioning indicator.

2.5 Normalization of R_s

The importance of the parameter R_s on regulating surface energy exchanges is well documented (Kelliher et al. 1995; Saigusa et al. 1998). Indeed, R_s depends significantly on the phenological responses to interannual and diurnal meteorological changes (Wilson and Baldocchi 2000; Li et al. 2006). However, R_s in the Penman–Monteith equation is an ill-defined quantity (see the discussion in Finnigan and Raupauch 1987; Baldocchi 1994) because R_s conceptually encompasses the entire surface boundary condition related to vapor transfer from land surface to atmosphere (see Fig. 1). Thus, it is difficult to directly measure R_s. In the practical application, R_s is usually derived by inverting Eq. 3 and using measured LE, R_a, and meteorological variables (Brutsaert 1982). Numerous previous modeling studies (e.g., Kelliher et al. 1995; Raupach 1995; Baldocchi and Meyers 1998) have shown that there exists a relationship between R_s and stomatal (physiological) resistance. However, R_s can also be affected by the non-physiological processes (Komatsu et al. 2005) because it is a parameter conceptualized to represent the entire vegetated surface rather than just the canopy or soil surface itself.

Wilson et al. (2002) showed a positive correlation between R_s and R_i for several types of vegetated surfaces. A high R_i under warm and dry atmospheric conditions induces a high R_s because of active physiological processes and increase in evaporation demand (Raupach 2000). Isaac et al. (2004) reported that R_s depends on several meteorological parameters as well as R_i, and Todorovic (1999) presented an evapotranspiration model of which the parameter R_s is normalized by R_i.

Based on the combined Penman–Monteith equation, a formula in which R_s depends on microclimatic variables has been introduced by Rana et al. (1997) as follows:

$$\frac{R_s}{R_a} = k_0 + k\sqrt{\frac{R_i}{R_a}} \tag{7}$$

where k_0 and k (dimensionless) in Eq. 7 are empirical calibration coefficients to be determined experimentally, both depend on plant physiology and soil water conditions (Rana et al. 1997; Perez et al. 1999). This empirical approach implies that R_s is proportional to $\sqrt{R_i R_a}$. In this paper, we denote $R_s/\sqrt{R_i R_a}$ as the "normalized R_s (R_s^*)" to identify the physiological process more clearly by eliminating the aerodynamic and meteorological effects on R_s of the entire surface. Eq. 5 can be mathematically converted to a linear equation containing the β and R_s^*:

$$\beta = mR_s^* - b, \ m = \frac{\sqrt{R_i R_a}}{(\varepsilon R_a + R_i)}, \ b = \frac{(R_i - R_a)}{(\varepsilon R_a + R_i)}, \tag{8}$$

$$R_s^* = \frac{R_s}{\sqrt{R_i R_a}}$$

This equation originated from the Penman–Monteith equation implies the relation of R_s^* to β. Therefore, in this study, we will analyze the processes of energy partitioning empirically by means of the R_s^* using Eq. 8.

3 Data

Baldocchi et al. (2001) emphasized the importance of conducting field experiments in various ecosystems with different land–atmosphere coupling characteristics. However, micrometeorological observational towers are distributed unevenly throughout the world. In an effort to compile surface flux data, the FLUXNET, as the "global network of regional networks," has been established to coordinate global analysis of the exchanges of carbon dioxide, water vapor and energy (Aubinet et al. 1999; Baldocchi et al. 2001). These exchanges are mainly governed by the partitioning of energy under different climatic and surface conditions. In response to temporal and spatial variations, the flux database updated from more than 500 FLUXNET tower sites (as of year 2010) across five continents are extending in terms of a long-term observation (http://www.daac.ornl.gov/FLUXNET/fluxnet.html). In addition, the FLUXNET sites typically measure not only flux data but also above-canopy meteorological data.

In this study, we used fluxes and meteorological data obtained from 25 FLUXNET sites over 60 site-years (see Table 1) as compiled by Wilson et al. (2002). Those sites are well known and discussed widely in the literature, among FLUXNET sites (e.g., Wilson and Baldocchi 2000; Wilson et al. 2002; Bonan 2008), and located in various vegetation types (e.g., deciduous forest, coniferous forest, grassland, Mediterranean, crop, and tundra) (see Fig. 2). The data compiled by Wilson et al. (2002) cover the periods ranging from late spring to summer (number of days: from 165 to 235), and they are limited only to daytime fluxes. The measured parameters were mean midday T_a, mean midday vapor pressure deficit, mean midday R_a, R_s and R_i, daytime α and β. R_s was calculated using the inverted Penman–Monteith equation during midday (from 1,000 to 1,430 local standard time). R_a was represented as the sum of u/u_*^2 (resistance to momentum transport), where u is the mean wind speed and u_* is the friction velocity. R_i was computed using midday estimation of δ_e and R_n (see Eq. 1). In the calculation of R_s and R_i, S and G are neglected for convenience because both are not substantial at most sites. In fact, there exists the useful approximation, $G+S=0.1\ R_n$. However, except R_n, G is governed by total plant area (Choudhury et al. 1987), and S is changed by total biomass, bole (or foliage) temperature, and canopy wetness (Aston 1985). Therefore, the ratio of $(G+S)$ to R_n will not be constant between sites having various vegetation types in this study. The cumulative β was evaluated from mean diurnal trend, excluding the nocturnal periods (see Wilson et al. (2002) for more details).

Eddy covariance system is strongly recommended by the FLUXNET since it is most direct micrometeorological technique for measuring surface energy fluxes (Meyers and Baldocchi 2005). However, measured fluxes usually do not show a closure of surface energy balance (Verma et al. 1986; Sánchez et al. 2010) even over relatively flat and homogeneous surfaces as well as short vegetation areas where are presumably an ideal condition for the application of eddy covariance method (Foken and Oncley 1995). Nevertheless, it would not affect our analysis results with β because previous studies reported the systematical underestimation of both H and LE by similar relative fractions at daytime (Turnipseed et al. 2002). Furthermore, in order to avoid the effect of underestimated LE in α (see Eq. 4), we recalculated α from Eq. 6 by using the information of site elevation, β and T_a data (see Appendix A) instead of α data compiled by Wilson et al. (2002). The values of α in Wilson et al. (2002) are slightly lower than the recalculated ones in this study (see Fig. 3), which is consistent with the tendency of underestimation of LE in the eddy covariance system.

Some recalculated α values are greater than 1.0. In fact, even though air passing over a wet surface may tend to become vapor saturated under the “minimal advection” conditions in the sense of λET_{equ} (Eq. 2), such conditions hardly ever occur due to the vertical transport of heat and water vapor caused by entrainment of dry air at the top of the convective boundary layer (Brutsaert 1982). In this case, λET will be in excess of λET_{equ} predicted by Eq. 2 (Priestley and Taylor 1972; McAneney and Itier 1996; Monteith and Unsworth 2008; Komatsu 2005).

4 Results and discussion

To demonstrate the influence of R_s on energy partitioning, Bagayoko et al. (2007) examined the relationship between β and surface conductance ($1/R_s$) and found a negative exponential relation between them. Similarly, in Fig. 4 constructed using Eq. 8, it shows that there exists a positive trend between β and R_s^* for various vegetated surfaces. β generally has a larger value for a smaller physiological activity of vegetation and relatively drier ground (a high R_s value) (Fraedrich et al. 1999). It is consistent with the positive trend of β and R_s^*. However, considering a negative relation between R_s^* and R_i in Eq. 8, the general behavior of R_i, a larger β value under a warmer and drier climate for high R_i (Beringer et al. 2005), does not contribute the positive trend in Fig. 4. R_a also cannot strongly lead the positive trend because of unclear relationship between β and R_a (see Eq. 5). Therefore, while the positive trend between β and R_s^* is strongly caused by the relationship between β and R_s, the relation between β and R_s^* is not exactly proportional due to the functions of R_i and R_a implied in R_s^*, particularly if β is larger than 1. In fact, microclimatic variables that are weather and canopy structure dependent affect not only the physical energy exchange but also the physiological behavior, and they have often been regarded as the main factor in determining the characteristics of energy partitioning in previous field experiments (e.g., Wilson et al. 2002). Thus, it is reasonable to express the slope (m) and intercept (b) of the linear Eq. 8 in terms of microclimatic parameters R_i and R_a.

Table 1 Summary of site information and tower measured parameters during the period between days 165 and 235 for each site year

Site	Year	V	Elev.	δ_e	T_a	ε	R_a	R_s	R_i	β	α
Harvard	1992	D	320	854	22.4	2.54	15	59	43	0.49	0.94
	1993	D	320	1,077	22.7	2.58	12	70	36	0.38	1.01
	1994	D	320	754	23.1	2.63	15	56	31	0.43	0.96
	1995	D	320	951	23.3	2.66	15	65	35	0.43	0.96
	1996	D	320	832	20.9	2.34	13	63	33	0.46	0.98
	1997	D	320	968	21.0	2.35	14	70	38	0.38	1.03
	1998	D	320	838	22.2	2.51	14	64	31	0.56	0.90
	1999	D	320	1,149	23.3	2.66	12	80	38	0.55	0.89
Walker Branch	1995	D	283	1,465	27.6	3.31	22	101	50	0.43	0.91
	1996	D	283	1,188	26.8	3.18	24	75	40	0.28	1.03
	1997	D	283	1,200	27.1	3.23	24	74	39	0.31	1.00
	1998	D	283	1,312	28.0	3.38	23	93	44	0.42	0.91
	1999	D	283	959	27.4	3.28	26	67	33	0.33	0.98
	2000	D	283	789	26.1	3.06	25	47	27	0.24	1.07
Gunnarsholt	1996	D	78	393	12.6	1.43	30	68	32	0.11	1.53
	1997	D	78	426	13.6	1.52	33	96	34	0.54	1.08
Tharandt	1996	C	380	995	19.3	2.16	13	82	40	0.69	0.87
	1997	C	380	803	17.4	1.95	11	81	33	0.75	0.86
	1998	C	380	1,028	19.0	2.13	12	96	41	0.76	0.84
Norunda	1996	C	43	973	18.0	1.94	13	94	45	0.79	0.85
	1997	C	43	1,333	21.4	2.33	13	132	53	0.9	0.75
	1998	C	43	743	16.9	1.82	12	74	39	0.54	1.01
Flakaliden	1996	C	226	891	17.3	1.90	19	105	42	0.79	0.85
	1997	C	226	1,027	18.6	2.04	23	151	45	1.07	0.72
	1998	C	226	563	15.0	1.67	18	70	31	0.9	0.84
WeidenBrunnen	1996	C	765	619	13.4	1.63	15	109	21	2.02	0.53
	1997	C	765	759	16.6	1.95	16	130	33	1.12	0.71
	1998	C	765	836	17.1	2.01	15	97	32	0.87	0.80
Hyytiälä	1996	C	170	689	16.2	1.78	17	88	33	0.64	0.95
Duke Forest	1998	C	176	1,874	29.1	3.53	17	178	67	0.65	0.78
	1999	C	176	2,076	30.9	3.86	18	142	66	0.52	0.83
Bordeaux	1996	C	60	1,787	25.3	2.86	16	157	63	1.18	0.62
	1997	C	60	1,315	25.3	2.86	17	81	49	0.46	0.92
North Boreas	1994	C	260	1,319	19.3	2.13	17	140	53	1.55	0.58
	1995	C	260	1,103	18.0	1.99	16	140	50	1.3	0.65
	1996	C	260	1,220	18.6	2.05	15	137	48	1.65	0.56
	1997	C	260	1,122	18.0	1.99	15	148	43	1.77	0.54
Aberfeldy	1997	C	340	652	16.0	1.79	21	190	36	2.2	0.49
	1998	C	340	625	14.7	1.67	18	177	36	1.92	0.55
Niwot Ridge	1999	C	859	910	14.8	1.78	17	81	33	0.86	0.84
Little Washit	1998	G	360	2,973	33.2	4.41	29	563	106	1.91	0.42
	1999	G	360	1,455	30.2	3.81	30	180	49	0.76	0.72
Shidler	1997	G	350	1,092	28.6	3.51	42	97	37	0.34	0.96
Fort Peck	1999	G	634	1,679	24.7	2.97	37	135	66	0.53	0.87
Blodgett Forest	1997	M	1,315	1,870	23.1	2.96	26	116	60	0.47	0.91
	1999	M	1,315	1,814	22.4	2.86	27	179	47	0.92	0.70
Metolius	1996	M	915	2,385	24.0	2.96	16	271	65	1.51	0.53
	1997	M	915	1,806	21.4	2.58	15	235	49	1.7	0.51
Castelporziano	1997	M	68	957	23.0	2.54	15	222	28	2.25	0.43

Table 1 (continued)

Site	Year	V	Elev.	δ_e	T_a	ε	R_a	R_s	R_i	β	α
Sky Oaks (O.)	1997	M	1,429	3,862	30.9	4.48	18	900	102	5.2	0.20
Sky Oaks (Y.)	1997	M	1,429	3,505	29.5	4.17	21	2,995	93	164.2	0.01
	1998	M	1,429	3,212	28.9	4.05	27	317	85	0.86	0.67
Bondville	1997	Cr	300	1,200	26.2	3.09	37	82	45	0.4	0.95
	1998	Cr	300	1,046	27.1	3.23	47	44	38	0.25	1.05
	1999	Cr	300	1,064	26.5	3.13	28	55	37	0.28	1.03
Happy Valley	1994	T	298	645	15.9	1.78	54	106	45	0.77	0.88
	1995	T	298	528	14.5	1.64	60	83	38	0.74	0.93
Atqasuk	1999	T	15	461	11.6	1.34	43	80	30	1.05	0.85
Barrow	1998	T	1	113	7.3	1.04	43	48	9	1.21	0.89
	1999	T	1	150	6.3	0.98	48	37	10	1.18	0.93

This table is basically modified from Tables 1 and 2 in Wilson et al. (2002). However, in this study, Elev. is cited from FLUXNET homepage, ε is recalculated (See Appendix A), and α is re-estimated using by Eq. 6

V vegetated lands, *D* deciduous forests, *C* coniferous forests, *G* grasslands, *M* Mediterranean climates, *Cr* crops, *T* Tundra, *Elev.* elevation (m), δ_e mean midday vapor pressure deficit (Pa), T_a mean midday air temperature (°C), ε Δ/γ calculated from T_a and Elev., R_a mean midday aerodynamic resistance (s m^{-1}), R_s bulk surface resistance (s m^{-1}), R_i climatology resistance (s m^{-1}), β the daytime Bowen ratio, α the daytime Priestly–Taylor coefficient

If the positive trend in Fig. 4 is represented using by a single linear regression, the correlation coefficient will be low with constant m and b values (β=0.21 R_s^*+0.01; R^2= 0.65). However, as plotted in Fig. 5, the relationship between m and T_a can be well represented by an exponential regression curve (R^2=0.97), especially when R_i is relatively high due to low actual water vapor pressure and R_a is low due to high aerodynamic transfer of vapor and heat. Generally, a higher temperature in the boundary layer implies greater average internal energy, mainly because that the transfer of heat energy to the boundary layer is influenced by T_a. Thus, the relation between β and R_s^* is governed by the amount of energy in the near-surface atmosphere. However, the energy fluxes in the near-surface boundary layer are also largely affected by the aerodynamic moment transfer. Therefore, the point with a relatively high R_a (low aerodynamic conductance) shows a deviation from the general pattern of the relation between T_a and m (as shown by the triangles in Fig. 5).

Assuming β approaches zero ($\beta\rightarrow0$), R_s^* in Eq. 8 approaches (R_i-R_a). Since both R_i and R_a have an influence on the surface boundary layer, (R_i-R_a) relates to T_a particularly at lower δ_e (cross marker shown in Fig. 6a). Furthermore, the quadratic relationship between T_a and (R_i-R_a) is more clear than that between R_i versus T_a (not shown here) although R_i has a theoretical relationship with T_a (see Eq. 1). Despite the fact that the aerodynamic roughness characteristics show no clear relationship with T_a (Mölder and Lindroth 1999), T_a has effects on R_a, apart from the extent of its influence, through the diffusion rate by the atmopsheric stability as the function of R_a (Verma 1989). At a higher δ_e, (R_i-R_a) positively increases with T_a since (R_i-R_a) is strongly controlled by the variation of R_i due to the much smaller value of R_a than R_i. Meanwhile, as an extension of the relationship between T_a and (R_i-R_a), $b\left(=\frac{(R_i-R_a)}{(\varepsilon R_a+R_i)}\right)$ has a quadratic relationship with T_a and mainly governed by R_a when R_i is lower than approximately 55 sm^{-1} (see

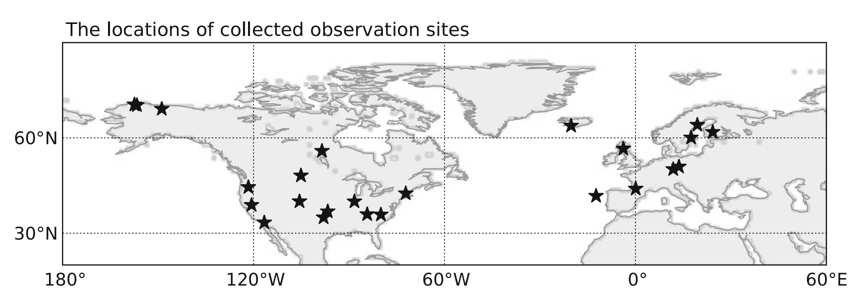

Fig. 2 The locations of 25 FLUXNET measurement sites used in this study (see Table 1)

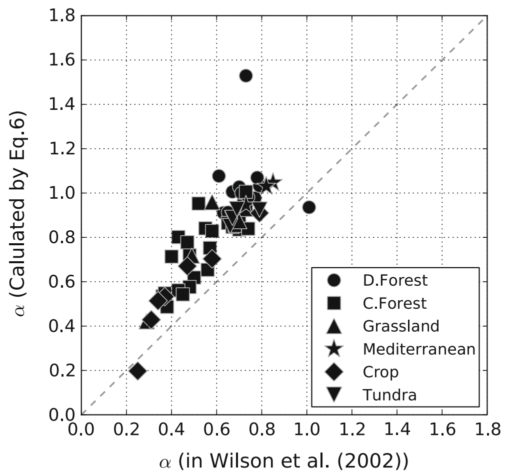

Fig. 3 Comparison of two estimates of the Priestley–Taylor coefficient (α). Measured α is taken from Wilson et al. (2002) ($\alpha = \frac{\lambda \mathrm{ET}}{\lambda \mathrm{ET}_{\mathrm{equ}}}$) while the one calculated is based on Eq. 6 of this study

Fig. 6b). However, when R_i is higher than ~55 sm^{-1}, b is relatively constant in a changing T_a (Fig. 6b).

Moreover, Figs. 5 and 6b consistently imply that the ratio of β to R_s^* is to a certain degree influenced by T_a, as well as Fig. 4. Under high (low) temperatures, β is less (more) sensitive to R_s^*, which is an indicative of vegetation physiological behaviors. The direct correlation between β and T_a is plotted in Fig. 7. According to Eq. 6, it can be expected that the relationship between β and T_a is negative because ε is a function of temperature. The relationship between β and T_a also depends on α (see Fig. 7): β is less (more) sensitive to T_a when α is high (low). In previous studies, α is mostly controlled by R_s. For example, Baldocchi (1994) showed that the dependence of α on R_s will change once a threshold value of R_s is exceeded. Monteith (1995) developed an empirical equation to estimate α by using the parameter R_s. Lhomme (1997) described α values of greater than 1.0 using the function of R_s/R_a to understand how the entrained energy cooperates

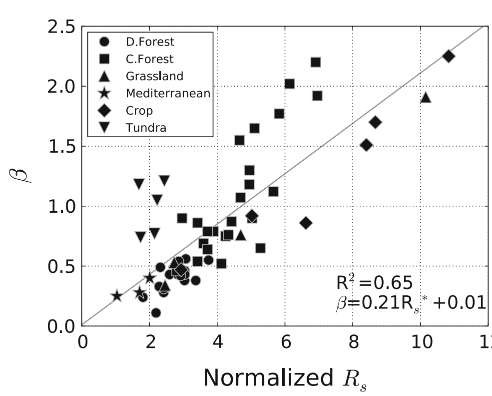

Fig. 4 Relationship between the normalized surface resistance (R_s^*) and Bowen ratio (β) for various vegetated surfaces

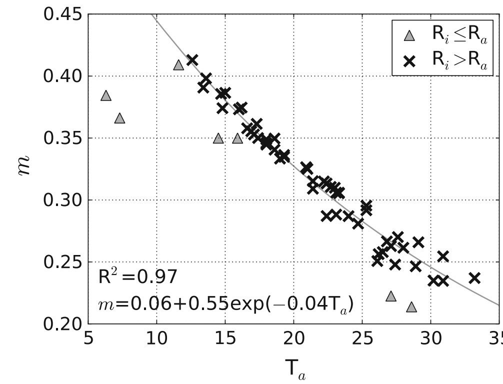

Fig. 5 Relationship between m in Eq. 8 and mean midday air temperature (T_a) for the data of $R_i \leq R_a$ (s m^{-1}) and $R_i > R_a$ (s m^{-1}), respectively. The exponential regression line is derived with respect to the data of $R_i > R_a$

with a conservative faction of A at the surface. In addition, R_s^* in this study also has a negative relationship with α, which indicates the land surface condition (see the exponential line in Fig. 8). Finally, we can also observe that the characteristics shown in Fig. 7 are similar to that obtained by using the proposed semi-empirical approaches defined by Eq. 8.

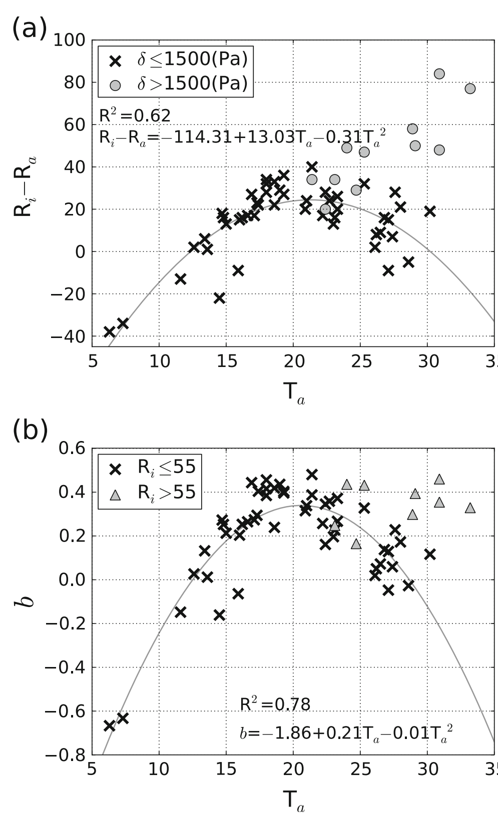

Fig. 6 **a** Relationship between (R_i–R_a) and mean midday air temperature (T_a) for $\delta_e \leq$1,500 Pa and $\delta_e >$1,500 Pa, respectively. **b** Behavior of b with respect to m in Eq. 8 for $R_i \leq$55 s m^{-1} and $R_i >$55 s m^{-1}. The second-order polynomial regression lines are derived with respect to the data of $\delta_e \leq$1,500 Pa

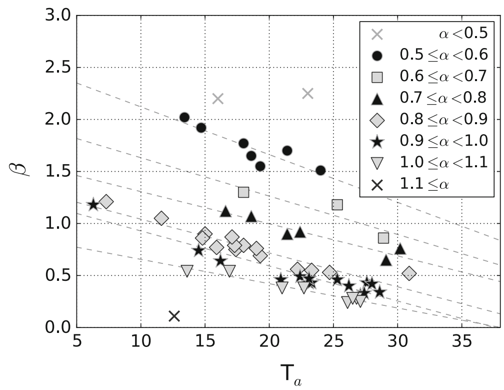

Fig. 7 Relationship between air temperature and Bowen ratio for different intervals of α. The linear regression lines follow are derived individually with respect to the data in each α interval

5 Conclusions

In this study, it is found that surface energy partitioning, as indicated by the Bowen ratio (β), is strongly governed by temperature. The sensitivity of energy to temperature is highly dependent on the surface conditions which can be expressed in terms of the normalized R_s ($R_s^* = \frac{R_s}{\sqrt{R_i R_a}}$) or the Priestley–Taylor coefficient (α). For a high R_s^* or a low α, the temperature sensitivity of β increases. In this case, high R_s^* and low α imply the boundary layer condition of a less vegetated surface, low vapor pressure deficit, low received radiative energy, and weak wind speed. Thus, warm environmental conditions in a well-watered reference surface involve relatively higher LE than H.

Owing to global warming effects, it is generally expected that warm air will become drier, and evaporation from terrestrial water storage will increase (Held and Soden 2006). However, observations over the past 50 years have revealed a decrease in terrestrial evaporation (Roderick and Farquhar 2004; Yang et al. 2006). Roderick and Farquhar (2002) attributed this to the decrease in the radiation received on the terrestrial surfaces. Decreased radiation generally results in low α (DeBruin and Keijman 1979; Sumner and Jacobs 2005), which produce higher sensitivity between T_a and β according to the result of this study. In other words, T_a has a critical effect on energy partitioning (i.e., β) under the boundary layer condition of low α that correspond to the wet vegetated surface and dry air condition (DeBruin and Keijman 1979; Crago 1996). In this study, a positive relationship between R_s^* and β is shown, and the sensitivity between them is found to be a function of T_a. In addition, a negative relationship between α and R_s^* is also represented. These relations among β, α, R_s^*, solar radiation, and T_a imply that the main evidence of recent LE change is not only caused by the radiation change but also by the changes in temperature and surface conditions.

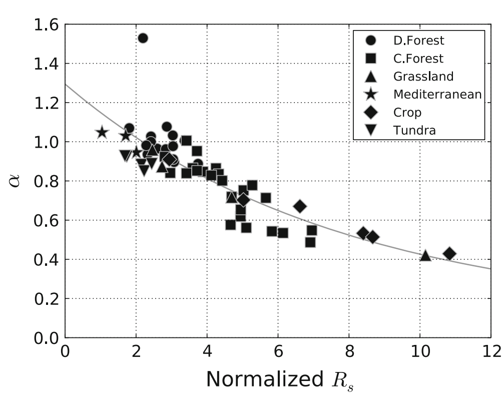

Fig. 8 Relationship between the normalized surface resistance (R_s^*) and the Priestley–Taylor coefficient (α) for various vegetated surfaces

It is important to understand the critical control of surface energy partitioning since LE is the single significant process in transporting heat and water vapor. A warmer atmosphere greatly enhances the partitioning of solar radiation into LE than a cooler atmosphere (Chang and Root 1975). The spatio-temporal effects of T_a on surface energy partitioning will be different according to the biome types and the climatic zones, as shown by our results. Our findings in this study are based on the data from only a limited amount of measurement sites. Further analyses of more available measurement data are necessary to identify more significant characteristics of the sensitivity of energy partitioning to T_a. It is anticipated that the empirical findings of this study will enhances scientific understanding of surface energy and water balance.

Acknowledgments We would like to thank editor and anonymous reviewers, whose comments were useful for revising this manuscript. This work was supported by JSPS KAKENHI, Grants-in-Aid for Scientific Research on Innovative Areas (22119009) and (S) (23226012), and Innovative program of climate change projection for the twenty-first century from The Ministry of Education, Culture, Sports, Science, and Technology (MEXT).

Appendix A

ε can represented by the ratio of Δ to γ. γ can be simply calculated with atmospheric pressure, P (Pa).

$$\gamma = \frac{C_p\, P}{R_{air}\, \lambda} = 664741.8P \tag{9}$$

where C_p is 1,013 (J kg^{-1}°C^{-1}) for moist air at constant pressure, λ is 2.45×10^{-3} (J kg^{-1}) at 20°C, and the ratio of molecular weight of water vapor divided by that of dry air

(R_{air}) is 0.622. P can be expressed with the elevation above the sea level z (m).

$$P = 101,300\left(\frac{293 - 0.0065z}{293}\right)^{5.26} \quad (10)$$

Moreover, Δ (Pa°C^{-1}) is the function of T_a (°C).

$$\Delta = \frac{4,098,000\left[0.6108\exp\left(\frac{17.27T_a}{T_a+237.3}\right)\right]}{\left(T_a+237.3\right)^2} \quad (11)$$

References

Admiral SA, Lafleur PM, Roulet NT (2006) Controls on latent heat flux and energy partitioning at a bog in eastern Canada. Agric For Meteorol 140:308–321

Aston AR (1985) Heat storage in a young eucalypt forest. Agric For Meteorol 35:281–297

Aubinet M, Grelle A, Ibrom A, Rannik Ü, Moncrieff J, Foken T, Kowalski AS, Martin PH, Berbigier P, Bernhofer Ch, Clement R, Elbers J, Granier A, Grünwald T, Morgenstern K, Pilegaard K, Rebmann C, Snijders W, Valentini R, Vesala T (1999) Estimates of the annual net carbon and water exchange of European forests: the EUROFLUX methodology. Advances in Ecological Research 30:113–175

Bagayoko F, Yonkeu S, Elbers J, van de Giesen N (2007) Energy partitioning over the West African savanna: multi-year evaporation and surface conductance measurements in Eastern Burkina Faso. J Hydrol 334:545–559

Baldocchi D (1994) A comparative study of mass and energy exchange over a closed C3 (wheat) and an open C4 (corn) canopy: I. The partitioning of available energy into latent and sensible heat exchange. Agric For Meteorol 67:191–220

Baldocchi DD, Meyers TP (1998) On using eco-physiological, micrometeorological and biogeochemical theory to evaluate carbon dioxide, water vapor and trace gas fluxes over vegetation: a perspective. Agric For Meteorol 90:1–25

Baldocchi D, Kelliher FM, Black TA, Jarvis P (2000) Climate and vegetation controls on boreal zone energy exchange. Glob Chang Biol 6:69–83

Baldocchi D, Falge E, Gu L, Olson R, Hollinger D, Running S, Anthoni P, Bernhofer Ch, Davis K, Evans R, Fuentes J, Goldstein A, Katul G, Law B, Lee X, Malhi Y, Meyers T, Munger W, Oechel W, Paw UKT, Pilegaard K, Schmid HP, Valentini R, Verma S, Vesala T, Wilson K, Wofsy S (2001) FLUXNET: a new tool to study the temporal and spatial variability of ecosystem-scale carbon dioxide, water vapor, and energy flux densities. Bull Am Meteorol Soc 82:2415–2434

Beljaars ACM, Holtslag AAM (1991) Flux parameterization over land surfaces for atmospheric models. J Appl Meteorol 30:327–341

Beringer J, Chapin FS III, Thompson CC, McGuire AD (2005) Surface energy exchanges along a tundra-forest transition and feedbacks to climate. Agric For Meteorol 131:143–161

Bonan GB (2002) Ecological climatology. Cambridge University Press, New York

Bonan GB (2008) Forests and climate change: forcings, feedbacks, and the climate benefits of forests. Science 320:1444–1449

Brutsaert W (1982) Evaporation into the atmosphere; theory, history, and application. Kluwer, Dordrecht

Chambers SD, Beringer J, Randerson JT, Chapin FS III (2005) Fire effects on net radiation and energy partitioning: contrasting responses of tundra and boreal forest ecosystems. J Geophys Res 110:D09106. doi:10.1029/2004JD005299

Chang JH, Root B (1975) On the relationship between mean monthly global radiation and air temperature. Archiv fur Meteorologie, Geophysik und Bioklimatologie, Ser B 23:13–30

Choudhury BJ, Idso SB, Reginato RJ (1987) Analysis of an empirical model for soil heat flux under a growing wheat crop for estimating evaporation by an infrared temperature based energy balance equation. Agric For Meteorol 39:283–297

Crago RD (1996) Comparison of the evaporative fraction and the Priestley–Taylor α for parameterizing daytime evaporation. Water Resources Research 32:1403–1409

DeBruin HAR, Keijman JQ (1979) The Priestley–Taylor evaporation model applied to a large, shallow lake in the Netherlands. Journal of Applied Meterology 18:898–903

DeHeer-Amissah A, Högström U, Smedman-Högström AS (1981) Calculation of sensible and latent heat fluxes, and surface resistance from profile data. Boundary-Layer Meteorology 20:35–49

Finnigan JJ, Raupauch MR (1987) Modern theory of transfer in plant canopies in relation to stomatal characteristics. In: Zeiger E, Farquhar G, Cowan L (eds) Stomatal function. Stanford University Press, Stanford, pp 385–429

Foken T, Oncley SP (1995) Results of the workshop "instrumental and methodical problems of land surface flux measurements. Bull Am Meteorol Soc 76:1191–1193

Fraedrich K, Kleidon A, Lunkeit F (1999) A green planet versus a desert world: estimating the effect of vegetation extremes on the atmosphere. J Clim 12:3156–3163

Hammerle A, Haslwanter A, Tappeiner U, Cernusca A, Wohlfahrt G (2008) Leaf area controls on energy partitioning of a temperature mountain grassland. Biogeosciences 5:421–431

Held IM, Soden BJ (2006) Robust responses of the hydrological cycle to global warming. J Clim 19:5686–5699

Henderson-Sellers A, Dickinson RE, Durbidge TB, Kennedy PJ, McGuffie K, Pitman AJ (1993) Tropical deforestation: modeling local- to regional-scale climate change. J Geophys Res 98:7289–7315

Holtslag AAM, Van Ulden AP (1983) A simple scheme for daytime estimates of the surface fluxes from routine weather data. J Clim Appl Meteorol 22:517–529

Isaac PR, Leuning R, Hacker JM, Cleugh HA, Coppin PA, Denmead OT, Raupach MR (2004) Estimation of regional evapotranspiration by combining aircraft and ground-based measurements. Boundary-Layer Meteorology 110:69–98

Jarvis PG, James GB, Landsberg JJ (1976) Coniferous forest. In: Monteith JL (ed) Vegetation and Atmosphere, vol 2. Academic, San Diego, pp 171–236

Kelliher FM, Leuning R, Raupach MR, Schulze ED (1995) Maximum conductances for evaporation from global vegetation types. Agric For Meteorol 73:1–16

Komatsu H (2005) Forest categorization according to dry-canopy evaporation rates in a growing season: comparison of the Priestley–Taylor coefficient values from various observation sites. Hydrol Process 19:3873–3896

Komatsu H, Kumagai T, Hotta N (2005) Is surface conductance theoretically independent of reference height? Hydrol Process 19:339–347

Komatsu H, Maita E, Otsuki K (2008) A model to estimate annual forest evapotranspiration in Japan from mean annual temperature. J Hydrol 348:330–340

Kondo J, Saigusa N, Sato T (1990) A parametrization of evaporation from bare soil surfaces. J Appl Meteorol 29:385–389

Lhomme J-P (1997) A theoretical basis for the Priestley–Taylor coefficient. Boundary-Layer Meteorology 82:179–191

Li SG, Eugster W, Asanuma J, Kotani A, Davaa G, Oyunbaatar D, Sugita M (2006) Energy partitioning and its biophysical controls above a grazing steppe in central Mongolia. Agric For Meteorol 137:89–106

McAneney KJ, Itier B (1996) Operational limits to the Priestley–Taylor formula. Irrig Sci 17:37–43

Meyers TP, Baldocchi DD (2005) Current micrometeorological flux methodologies with application in agriculture. In: Hatfield, J.L., Baker, J.M., Viney, M.K. (eds) Micrometeorology in Agricultural Systems, Agronomy Series 47. American Society of Agronomy, Inc.; Crop Science Society of America, Inc.; Soil Science Society of America, Inc., Madison, Wisconsin, USA, pp. 381–396.

Mölder M, Lindroth A (1999) Thermal roughness length of a boreal forest. Agric For Meteorol 98–99:659–670

Mölders N (2005) Plant- and soil-parameter-caused uncertainty of predicted surface fluxes. Mon Weather Rev 133:3498–3516

Monteith JL (1965) Evaporation and Environment. In: Proceedings of the 19th symposium of the society for experimental biology. Cambridge University Press, New York

Monteith JL (1995) Accommodation between transpiring vegetation and the convective boundary layer. J Hydrol 166:251–263

Monteith JL, Unsworth MH (2008) Principles of Environmental Physics, 3rd edn. Academic, San Diego

Perez PJ, Castellvi F, Rosell JI, Ibañez M (1999) Assessment of reliability of Bowen ratio method for partitioning fluxes. Agric For Meteorol 97:141–150

Priestley CHB, Taylor RJ (1972) On the assessment of surface heat flux and evaporation using large-scale parameters. Mon Weather Rev 100:81–92

Rana G, Katerji N, Mastrorilli M, El Moujabber M, Brisson N (1997) Validation of a model of actual evapotranspiration for water stressed soybeans. Agric For Meteorol 86:215–224

Randall DA et al (2007) Climate models and their evaluation. In: Solomon S, Qin D, Manning M, Chen Z, Marquis M, Averyt KB, Tignor M, Miller HL (eds) Climate change 2007: the physical science basis. Contribution of Working Group I to the Fourth Assessment Report of the Intergovernmental Panel on Climate Change. Cambridge University Press, Cambridge

Raupach MR (1995) Vegetation–atmosphere interaction and surface conductance at leaf, canopy and regional scale. Agric For Meteorol 73:151–179

Raupach MR (2000) Equilibrium evaporation and the convective boundary layer. Boundary-Layer Meteorology 96:107–141

Roderick ML, Farquhar GD (2002) The cause of decreased pan evaporation over the past 50 years. Science 298:1410–1411

Roderick ML, Farquhar GD (2004) Changes in Australian pan evaporation from 1970 to 2002. Int J Climatol 24:1077–1090

Saigusa N, Oikawa T, Liu S (1998) Seasonal variations of the exchange of CO_2 and H_2O between a grassland and the atmosphere: an experimental study. Agric For Meteorol 89:131–139

Sánchez JM, Caselles V, Rubio EM (2010) Analysis of the energy balance closure over a FLUXNET boreal forest in Finland. Hydrology and Earth System Sciences 14:1487–1497

Sumner DM, Jacobs JM (2005) Utility of Penman–Monteith, Priestley–Taylor, reference evapotranspiration, and pan evaporation methods to estimate pasture evapotranspiration. J Hydrol 308:81–104

Thom AS (1975) Momentum, mass and heat exchange of plant communities. In: Monteith JL (ed) Vegetation and the atmosphere, vol 1, Principles. Academic, London, pp 57–109

Todorovic M (1999) Single-layer evapotranspiration model with variable canopy resistance. J Irrig Drain Eng 125:235–245

Trenberth KE et al (2007) Observations: surface and atmospheric climate change In: Solomon S, Qin D, Manning M, Chen Z, Marquis M, Averyt KB, Tignor M, Miller HL (eds) Climate change 2007: the physical science basis. Contribution of Working Group I to the Fourth Assessment Report of the Intergovernmental Panel on Climate Change. Cambridge University Press, Cambridge

Turnipseed AA, Blanken PD, Anderson DE, Monson RK (2002) Energy budget above a high elevation subalpine forest in complex topography. Agric For Meteorol 110:177–201

Verma SB (1989) Aerodynamic resistances to transfers of heat, mass and momentum. In: T. A. Black, D. L. Spittlehouse, M. D. Novak, and D. T. Price (eds) Estimation of areal evapotranspiration. International Association of Hydrological Sciences. pp 13–20.

Verma AB, Baldocchi DD, Anderson DE, Matt DR, Clement RJ (1986) Eddy fluxes of CO_2, water vapor, and sensible heat over a deciduous forest. Boundary-Layer Meteorology 36:71–91

Wilson KB, Baldocchi DD (2000) Seasonal and interannual variability of energy fluxes over a broadleaved temperate deciduous forest. Agric For Meteorol 100:1–18

Wilson KB, Baldocchi DD, Aubient M, Berbigier P, Bernhofer C, Dolman H, Falge E, Field C, Goldstein A, Katul G, Law BE, Lindroth A, Meyers T, Moncrieff J, Monson R, Oechel W, Tenhunen J, Valentini R, Verma S, Vesala T, Wofsy S (2002) Energy partitioning between latent and sensible heat flux during the warm season at FLUXNET sites. Water Resources Research 38:1294. doi:10.1029/2001WR000989

Yang D, Sun F, Liu Z, Cong Z, Lei Z (2006) Interpreting the complementary relationship in non-humid environments based on the Budyko and Panman hypotheses. Geophys Res Lett 33: LI8402. doi:10.1029/2006GL027657